Tropospheric emission spectrometer (TES) and atmospheric chemistry experiment (ACE) measurements of tropospheric chemistry in tropical southeast Asia during a moderate El Niño in 2006

Curtis P. Rinsland[a],*, Ming Luo[b], Mark W. Shephard[c], Cathy Clerbaux[d],
Chris D. Boone[e], Peter F. Bernath[e,f], Linda Chiou[g], P.F. Coheur[h]

[a]NASA Langley Research Center, Science Directorate, Mail Stop 401A, Hampton, VA 23681-2199, USA
[b]Jet Propulsion Laboratory, California Institute of Technology, 4800 Oak Grove Drive, Pasadena, CA 91109 USA
[c]Atmospheric and Environmental Research, Inc. (AER), 131 Hartwell Avenue, Lexington, MA 02421-3126, USA
[d]Service d'Aéronomie/IPSL, CNRS, Université Paris6, BP102, 4 Place Jussieu, 75252, Paris, France
[e]Department of Chemistry, University of Waterloo, Waterloo, Ontario, Canada N2L 3G1
[f]Department of Chemistry, University of York, Heslington, York YO10 5DD, United Kingdom
[g]Science Systems and Applications, Inc., 1 Enterprise Parkway, Suite 200, Hampton, VA 23666 USA
[h]Spectroscopie de l'Atmosphère, Chimie Quantique et Photophysique CP 160/09, Université Libre de Bruxelles, 50 Avenue, F.D. Roosevelt,
B-1050 Brussels, Belgium

Abstract

High spectral resolution Fourier transform spectrometer (FTS) measurements of tropospheric carbon monoxide (CO) distributions show mixing ratios over Indonesia during October 2006 of $\sim$200 ppbv (10^{-9} per unit volume) in the middle troposphere. The elevated emissions were caused by intense and widespread Indonesian peat and forest fire emissions elevated compared to other years by the impact of a moderate El Niño/Soutern Oscillation (ENSO) event, which delayed that year's monsoon season and produced very dry conditions. Moderate resolution imaging spectrometer (MODIS) fire counts, atmospheric chemistry experiment (ACE) measurements of elevated mixing ratios of fire emission products and near infrared extinction, and back trajectory calculations for a sample measurement location near the time of maximum emissions provide additional evidence that the elevated 2006 emissions resulted primarily from the Indonesia fires. Lower CO mixing ratios measured by ACE and fewer MODIS fire counts in Indonesia during October 2005 indicate lower emissions than during 2006. Coincident profiles from the ACE agree within the uncertainties with those from the tropospheric emission spectrometer (TES) for pressure ranges and time periods with good TES sensitivity after accounting for its lower vertical sensitivity compared with the ACE FTS.
© 2007 Elsevier Ltd. All rights reserved.

Keywords: Remote sensing; Tropospheric chemistry; Pollution; Spectroscopy; Carbon monoxide

*Corresponding author. Tel.: +1 757 8642699; fax: +1 757 8648197.
E-mail addresses: curtis.p.rinsland@nasa.gov (C.P. Rinsland), ming.luo@jpl.nasa.gov (M. Luo), mshephar@aer.com (M.W. Shephard), catherine.clerbaux@aero.jussieu.fr (C. Clerbaux), cboone@sciborg.uwaterloo.ca, cboone@acebox.uwaterloo.ca (C.D. Boone), bernath@uwaterloo.ca, pfb500@york.ac.uk (P.F. Bernath), linda.s.chiou@nasa.gov (L. Chiou), pfcoheur@ulb.ac.be (P.F. Coheur).

1. Introduction

The purpose of this paper is to report satellite-based measurements of tropospheric chemistry from the tropospheric emission spectrometer (TES) [1,2] and the atmospheric chemistry experiment (ACE) [3] with a primary focus on carbon monoxide (CO). The two instruments were selected for analysis and comparison of results because they both provide high precision measurements from high spectral resolution Fourier transform spectrometers (FTSs), though with different measurement and retrieval techniques. Nonlinear least squares spectral fitting of the target molecule and interferences in microwindows over a pre-selected altitude range [4] with a modified global fit approach [5] is used in the analysis of the solar occultation spectra recorded by the ACE FTS. The emission spectra recorded by the TES FTS are analyzed with the optimal estimation method [6] to yield profile inversions also with pre-selected microwindows and fitting of interferences. Although the TES FTS was designed to record both nadir and limb emission spectra [1,2], nadir measurements are now primarily recorded and those results are considered here. The sensitivity of TES CO measurements has been improved since shortly after launch [7], and we compare CO profiles from the TES instrument for a time period of improved results at pressure ranges of good sensitivity taking into account its lower vertical resolution in a comparison of those results with coincident profiles measured by the ACE FTS.

Enhancements in CO during northern hemisphere autumn 2006 relative to measurements from the same season in 2005 were caused primarily by intense peat and forest fire emissions in Indonesia. Tropical peatland forests and swamplands are one of the largest near-surface reserves of terrestrial organic carbon, and hence their stability is important, particularly as drainage, forest clearing and droughts become more common with important implications for climate change [8]. Emissions from fires occur in Indonesia during the dry season every year but were made worse in 2006 by a moderate El Niño/Soutern Oscillation (ENSO) event, which delayed the year's monsoon season due to sharply reduced rainfall beginning in July. The change in the weather pattern allowed wildfires across the dense tropical rainforests of Sumatra, Kalimantan, and Malaysia to spread rapidly with a rise in wildfire activity in on that region that was the worst since the intense 1997–98 El Niño event with fires in Kalimantan, Borneo, producing great amounts of smoke and elevated regional haze [9]. Fig. 1 illustrates moderate resolution imaging spectrometer (MODIS) fire counts for the Indonesian region ($15°S$–$15°N$ and $60°E$–$180°E$) from May–December 2005 and 2006. The time series illustrate the factor of three higher 2006 fire count maximum near the October maximum.

The importance and role of CO in tropospheric chemistry and climate is well established [10–15] with many studies since its first measurement from ground-based solar spectra in 1950–1951 [16]. It has potentially serious impacts on humans and animals when elevated. It is an odorless, colorless, and toxic gas and in the presence of nitrogen oxides (NO_x) it is either a source or a sink of tropospheric ozone. CO is the by-product of fossil fuel use, which is the dominant source at northern mid-latitudes, while the main sources in the tropics are oxidation of CH_4 and biogenic nonmethane hydrocarbons, and biomass burning. Reaction with the hydroxyl radical (OH) is the main removal process for CO, as it is for many other atmospheric species with CO an important sink for OH. CO consumes a large fraction of the OH in the troposphere. The lifetime of CO varies with altitude, latitude, and season and is on average about 2 months, long enough to allow intercontinental transport and cause hemispheric-scale air pollution. CO and ozone are two of the pollutants monitored for air quality by the US Environmental Protection Agency (EPA) and both are now measured globally and simultaneously by the TES instrument.

The TES and ACE instruments are among those currently providing global measurements of CO from space. Other satellite instruments also measuring global distributions of CO include the nadir-viewing measurement of pollution in the troposphere (MOPITT) onboard the Earth observing system (EOS) Terra (AM-1) platform [10,15,17–19], the nadir-viewing atmospheric infrared sounder (AIRS) instrument onboard the EOS Aqua platform [20,21], the nadir- and limb-viewing UV/visible/near-infrared scanning imaging absorption spectrometer for atmospheric chartography (SCIAMACHY) instrument onboard the European environmental ENVISAT 1 platform [22–24], the limb-viewing Michelson interferometer for passive remote sensing (MIPAS) also aboard ENVISAT 1 [25], the EOS Aura microwave limb sounder (MLS) [26,27] onboard the EOS Aura platform, and the nadir-viewing infrared atmospheric sounding interferometer (IASI) [28] recently launched onboard the METOP series of European meteorological satellites.
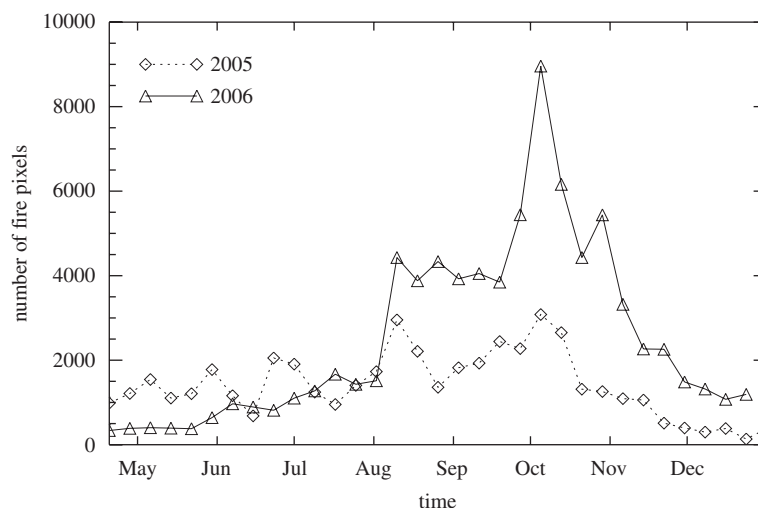
Fig. 1. Moderate resolution imaging spectrometer (MODIS) fire counts for 8 day increments covering the Indonesian region (15S°-15°N and 60°E-180°E) for the May–December time period during 2005 and 2006.

2. TES Measurements and CO Retrievals

The TES was launched on NASA's EOS Aura satellite on July 15, 2004 and placed in a near-polar orbit at an altitude of 705 km [29]. TES is providing continuous global observations of tropospheric CO, O_3, H_2O, CH_4, and temperature [1,2]. Spectral windows for the retrieval of CO were selected based on sensitivities calculated for TES filter 1A1 (1890–2260 cm^{-1}) where the CO (1–0) band is located [7]. An evaluation of errors calculated for northern mid-latitude conditions indicates a DOF of 0.8 for TES CO [30]. TES nadir measurements are recorded at 0.06-cm^{-1} spectral resolution (8.33 cm maximum optical path difference derived from double-sided interferograms) with a 16-pixel footprint of 5×8 km [7]. The TES forward model includes modeling of the water vapor continuum with a climatological CO_2 mixing ratio profile [31]. The TES retrieval algorithm estimates an atmospheric profile by simultaneously minimizing the difference between observed and model spectral radiances subject to the constraint that the solution is consistent with an *a priori* mixing ratio profile within covariance constraints [32,33].

Measured radiances are compared with those calculated for the same location with the TES forward model. The measured radiances are apodized with Norton–Beer strong apodization [34]. As clouds are often present in the troposphere and substantially affect the radiances measured by TES, an algorithm is used to quantify how clouds impact the measured optical depths in the spectral windows selected for retrieving temperature and gas constituent profiles [35]. The approach is to retrieve a single layer cloud that is coarsely spaced in wavenumber by 25–100 cm^{-1} with an effective optical depth that accounts both for cloud absorption and scattering. The cloud is assumed to have an effective height and a Gaussian profile in altitude, and effective cloud thickness. No scattering is assumed. Comparisons of TES retrievals for these parameters to model fields and selected measurements were found not to introduce observable biases in the TES retrievals, though CO was not considered in the analysis. Characterization of TES retrieval information content includes the quantification of smoothing, "cross-state", and systematic errors [32]. All parameters are derived from a simultaneous analysis of the measured spectrum.

Spectroscopic parameters assumed by TES version 2 retrievals were taken from the 2000 HITRAN (high resolution transmission) database with updates through September 2001 [36], though further updates from HITRAN 2004 [37] have been incorporated and are used in the forward model calculations and analysis. Similar to most other experiments operating in the infrared, TES uses spectral windows to limit the impact of spectroscopic errors of interfering species in the retrievals from 11 windows between 2086.06 and 2176.66 cm^{-1}. Temperature and interferences fitted for all windows are N_2O, CO_2, O_3, and H_2O [7] CO profiles are retrieved after temperature, ozone, and water vapor profiles are fitted in addition to the interferences.

Early TES CO results were affected by changes in instrument alignment as a function of time [7]. A useful value calculated from the information about the measurement and the *a priori* data is the degrees of freedom (DOF) for signal that describes the number of independent pieces of information available in the retrieved vertical profile [6,7,32]. Shortly after launch, the measured DOF for TES CO signal typically varied from 0.5–1.5, high in tropics with values up to two and gradually dropping below 0.5 at high latitudes. As the signal strength of 1A1 filter became weaker from end of 2004 to November 2005, the DOF for TES CO gradually declined. The optical bench warm up of ~5 K (November 29–December 2, 2005) improved TES signal-to-noise ratios so the DOF for CO increased to an averaged value of 1.45 (from the pre-warm-up value of 0.72) with many values now greater than 2.0 at 30°S–30°N. In addition, periodically (over 10 times thus far), detector temperatures have been raised to de-ice them. Although error in the temperature retrieval propagates into the error for CO, it is small compared to the other sources of error. A time sequence of TES average DOF for CO retrievals at 30°N–30°S illustrated the changes in sensitivity from launch through April 20, 2006 (Fig. 1 of Ref. [7]).

Similar to MOPITT [10,17–19], TES CO profile measurements are highly correlated vertically, with about 1–2 pieces of independent vertical information for each sounding. Random error due to instrument noise with a value of 5–10% is lower than the smoothing error in most places. Systematic error due to errors in the HITRAN spectroscopic parameters [36,37] and the cross-state error terms are small components in the error budget. The smoothing error is the largest component (10–20%), with the total relative error (~20–30%) combined from the random, the smoothing, the systematic, and the cross-state errors [32].

Current TES CO retrievals assume *a priori* profiles given by the model for ozone and related chemical tracers (MOZART) chemical transport model [38]. Monthly mean mixing ratios in 10° latitude by 60° longitude bins are used to create the *a priori* profiles assumed for TES retrievals with an altitude-dependent Tikhonov constraint [33]. In contrast, the MOPITT analysis relies on a single *a priori* profile and covariance matrix for CO retrievals [10]. MOPITT achieves near-complete global coverage in 3 days [39]. The impact of the different *a priori* constraints on TES and MOPITT retrievals has been described and characterized [39] based on the formalism of Rodgers and Connor [40].

3. ACE measurements and CO retrievals

Three instruments onboard SCISAT-1 share a common field of view taking advantage of the high precision of the solar occultation technique [3,4]. Measurements of CO are recorded with the FTS below about 105 km altitude at 0.02 cm^{-1} spectral resolution (maximum optical path difference of ± 25 cm) from 750 to 4400 cm^{-1}. Full-resolution spectra are recorded in 2 s with an altitude spacing determined by the scan time, typically 3–4 km, varying from 2 km for long, high beta angle (angle between the satellite velocity vector and the vector towards the Sun) occultations and up to 6 km for zero beta angle occultations in the absence of refraction. As a result of refraction, tangent altitude spacing is typically less than 2 km in the troposphere. The FTS has a circular field of view with 1.25 mrad diameter, which corresponds to a field of view of about 4 km at the limb in the absence of refraction. Photovoltaic detectors with near linear response are cooled to less than 100 K producing a signal-to-noise ratio of >300 throughout most of the spectral range. Low Sun solar occultation spectra are divided by exo-atmospheric solar spectra from the same occultation. The ACE orbit yields solar occultation measurements between 85°N and 85°S latitude. The orbit is optimized for high latitude occultation coverage with measurements at middle and low latitudes recorded only over limited time spans and a latitudinal coverage that changes rapidly with time. The orbit produces limited measurements during June and December when there is a high beta measurement period of about 3 weeks with no occultations. The current version of ACE FTS measurements (version of 2.2) provides mixing ratio profiles of over two dozen species in addition to CO with altitude coverage that depends on the species. Additional instruments onboard are a UV-visible spectrometer (MAESTRO, (measurement of aerosol extinction in the stratosphere and troposphere by occultation), a two channel UV-visible spectrophotometer, and two imagers with optical filters at 0.525 ± 1 and 1.02 ± 1 μm.

Version 2.2 profiles with statistical uncertainties are retrieved for individual molecules from fits to multiple species in pre-selected microwindows over pre-specified altitude ranges [4]. The global-fit non-linear least squares approach adopted by ACE is similar to the approach used previously by the atmospheric trace

molecule spectroscopy (ATMOS) experiment [41]. ACE temperature profiles are retrieved assuming a realistic CO_2 volume mixing ratio profile accounting for its increase as a function of time. Profiles are retrieved from fits to measurements in microwindows selected to provide CO_2 lines covering a wide range of sensitivities with respect to temperature and are constrained to yield an atmosphere in hydrostatic equilibrium. Retrievals below 12 km altitude assume temperatures derived by the Canadian Meteorological Centre (CMC) for the location of the observation. As shown from statistics based on 10 years of SAGE (Stratospheric Aerosol and Gas Experiment) II occultation measurements with a similar field of view as the ACE FTS, occultation measurements penetrate ~5 km below the tropopause 50% of the time at all latitudes [42]. However, although there are a few exceptions, the ACE measurements for the 2006 Indonesian fire time period were limited to a minimum altitude of ~8 km, probably due to the intense smoke and haze generated by the fires.

Spectroscopic line parameters and cross sections from HITRAN 2004 [37] have been assumed. Retrievals from ACE are obtained from both the strong (1–0) vibration–rotation band at 4.3 μm and the weaker (2–0) band at 2.3 μm. The weaker band provides tropospheric profiles above cloud tops from a spectral region primarily impacted by interfering absorptions by CH_4 lines. The MOPITT instrument was also designed to measure both bands [19], but the (2–0) band was not used in MOPITT operational retrievals due to the limited sensitivity achieved by the instrument in that spectral region. Averaging kernels for microwindows in the (2–0) band used by ACE for tropospheric measurements are sharply peaked with a full-width at half-maximum of 2 km or less in the troposphere [43].

4. TES-ACE CO measurement comparison

Direct comparison between TES and ACE CO profile retrievals is not proper due to the differences in the sensitivities of the two instruments. The *a priori* profiles and error covariances of the two instruments are not the same. Rodgers and Connor [40] derived an equation to adjust a retrieved profile for a different *a priori* profile and error covariance constraints. Here we adjust the ACE measured CO mixing ratio $X_{(ACEmeas)}$ to the TES *a priori* profile $X_{(TESapr)}$ via the following equation,

$$X_{(ACEadj)} = X_{(TESapr)} + A_{(TES)} \quad [(X(ace)_{map} - X_{(TESapr)}],\tag{1}$$

where $X_{(TESapr)}$ is the TES *a priori* profile, $A_{(TES)}$ is the TES averaging kernel matrix, and $X(ace)_{map}$ is the ACE mixing ratio mapped on to the TES vertical grid. We note the assumption in the comparison is that ACE has a vertical resolution much greater than the other (TES) instrument, which is 5–10 km depending on the latitude and season. The comparison is only valid for the altitude range within which the averaging kernels of both instruments are significant. Both approximations are assumed for this comparison. Before the mapping, the ACE CO profiles were extended downward to the surface via the shifted ACE first guess profile. The same approach has been used in comparing TES CO measurements with those from MOPITT [39] and differential absorption CO measurement (DACOM) spectrometer aircraft measurements during the Intercontinental Chemical Transport (INTEX)-B campaign [44].

Measurements from ACE and TES have been compared based on 24 h, 300 km maximum distance coincidence criteria after adjustment with Eq. (1). Version 2.2 ACE measurements with 1 km altitude spacing and version 2 TES measurements have been used. A preliminary Aura validation comparisons reported from MLS measurements assumed coincidence criteria of same day, 12° longitude [27].

Fig. 2 compares average coincident CO distributions at 200 to 600 hPa measured by TES and ACE during January–December 2006. We restrict the comparisons to 2006 when TES had improved CO sensitivity. Columns left to right show the TES and ACE retrieved mixing ratio, the TES and ACE CO profile with the TES averaging kernel and *a priori* applied to adjust ACE profiles to the TES vertical resolution including only measurements where the sum of the rows of the averaging kernels >0.7, the ACE minus TES difference, the averaging kernel value, and the total number of observations. The rightmost panel depicts TES sensitivity for the pressure range 200–600 hPa. Each profile for which the sum of the rows of the averaging kernels exceeds 0.7 within 200–600 hPa is included. TES measurements above ~200 hPa reflect a loss of sensitivity and are primarily from the *a priori* CO profile assumed from the MOZART model [38]. The number of coincidences decreases below 20 km primarily due to the limited number of ACE clear sky views, particularly at the lowest altitude. The results show that application of the TES averaging kernels and the *a priori* vector produced CO
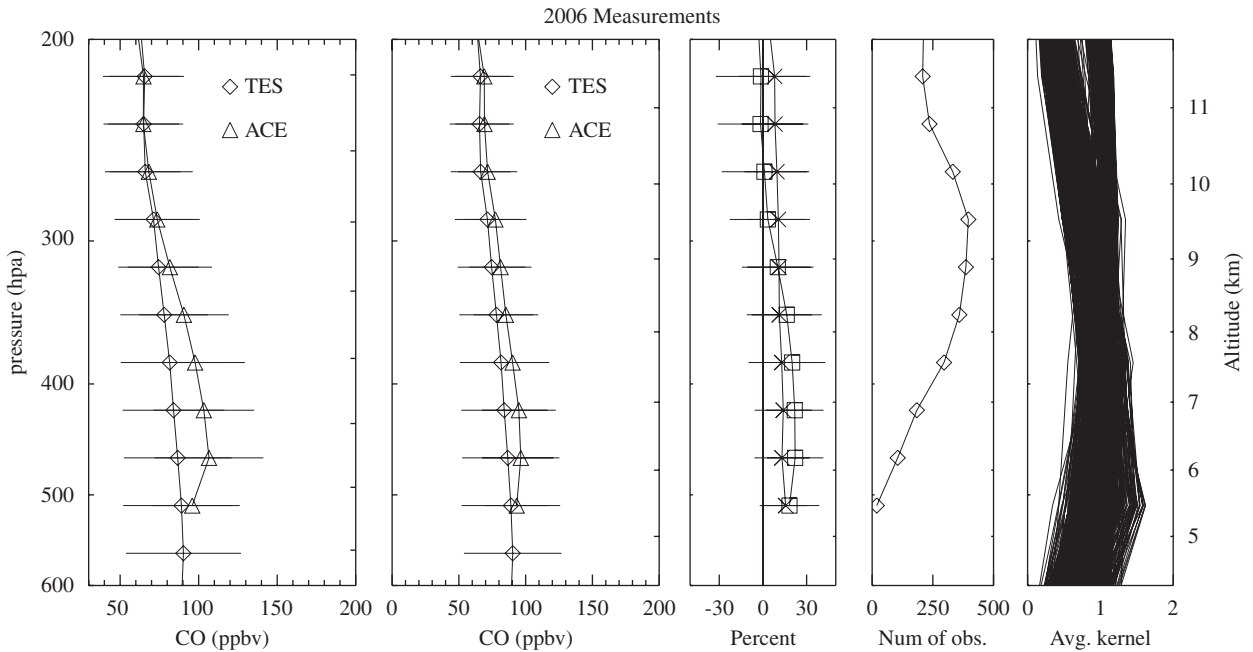
Fig. 2. Columns left to right show the measured mixing ratios (with standard deviations as horizontal lines), the adjusted mixing ratio (with standard deviations as horizontal lines), the ACE minus TES differences, the total number of observations, and the averaging kernel. Difference reported in the third column is calculated in percent with the formula ((ACE mixing ratio−TES mixing ratio)/base) × 100), where base is defined as the mean of the TES and ACE mixing ratios. The rightmost panel depicts TES sensitivity for the pressure range 200–600 hPa. Approximate altitudes are shown on the far right vertical axis.

profiles with better agreement for levels with good sensitivity. This improvement is due to the removal of the influence of the *a priori* assumptions in the TES CO profiles and the degradation of ACE vertical resolution to that of the TES instrument. Differences (ACE minus TES) and the number of coincidences with standard deviations are $(12.4 \pm 23.0)\%$ with 300 coincidences at 383 hPa, $(13.1 \pm 19.5)\%$ with 195 coincidences at 421 hPa, $(12.2 \pm 18.9)\%$ with 112 coincidences at 464 hPa, and $(16.1 \pm 14.4)\%$ with 20 coincidences at 510 hPa. As mentioned previously, early TES measurements recorded prior to implementation of the optical bench warm up are excluded because of their lower sensitivity [7].

Fig. 3 illustrates September to December 2006 monthly mean TES CO mixing ratios at 464 and 215 hPa for latitudes of 15°S to 15°N and longitudes from 60°E to 180°E with corresponding MODIS fire pixel counts for the same months. Monthly mean TES CO mixing ratios of ~200 ppbv were measured over Borneo and Sumatra during the time period of maximum emissions during October and November 2006. The monthly mean mixing ratio at 464 and 215 hPa during October 2006 were 288 and 198 ppbv, respectively, while maximum monthly mean mixing ratio at the same two pressure levels for November were 254 and 215 ppbv at the same pressure levels with a factor of two lower CO mixing ratios measured in December. The high MODIS pixel counts over Borneo and Sumatra during October 2006 indicate that fires were the primary cause of the increased CO and tropospheric O_3 emissions noted previously [45]. Wildfires across the dense tropical rainforests of Sumatra, Kalimantan, and Malaysia spread quickly [9]. The impact of the 2006 fires was significantly weaker than from tropical fire emissions over southeast Asia in 1997–1998. Measurements of CO by TES from 2005 are not shown because they were recorded prior to full implementation of the optical bench warm up [7].

The orbit selected for ACE repeats and is optimized for high latitude coverage in both hemispheres [3] with measurements over the Indonesian region only during limited time periods each year. Fig. 4 illustrates ACE version 2.2 measurements of CO tropical and subtropical profiles measured during October 2005 and October 2006 (15°S–15N° latitude, 60°E–180E° longitude) covering the same region as in Fig. 3. The left panel shows the mixing ratios versus altitude with horizontal lines showing the standard deviations from each of the two
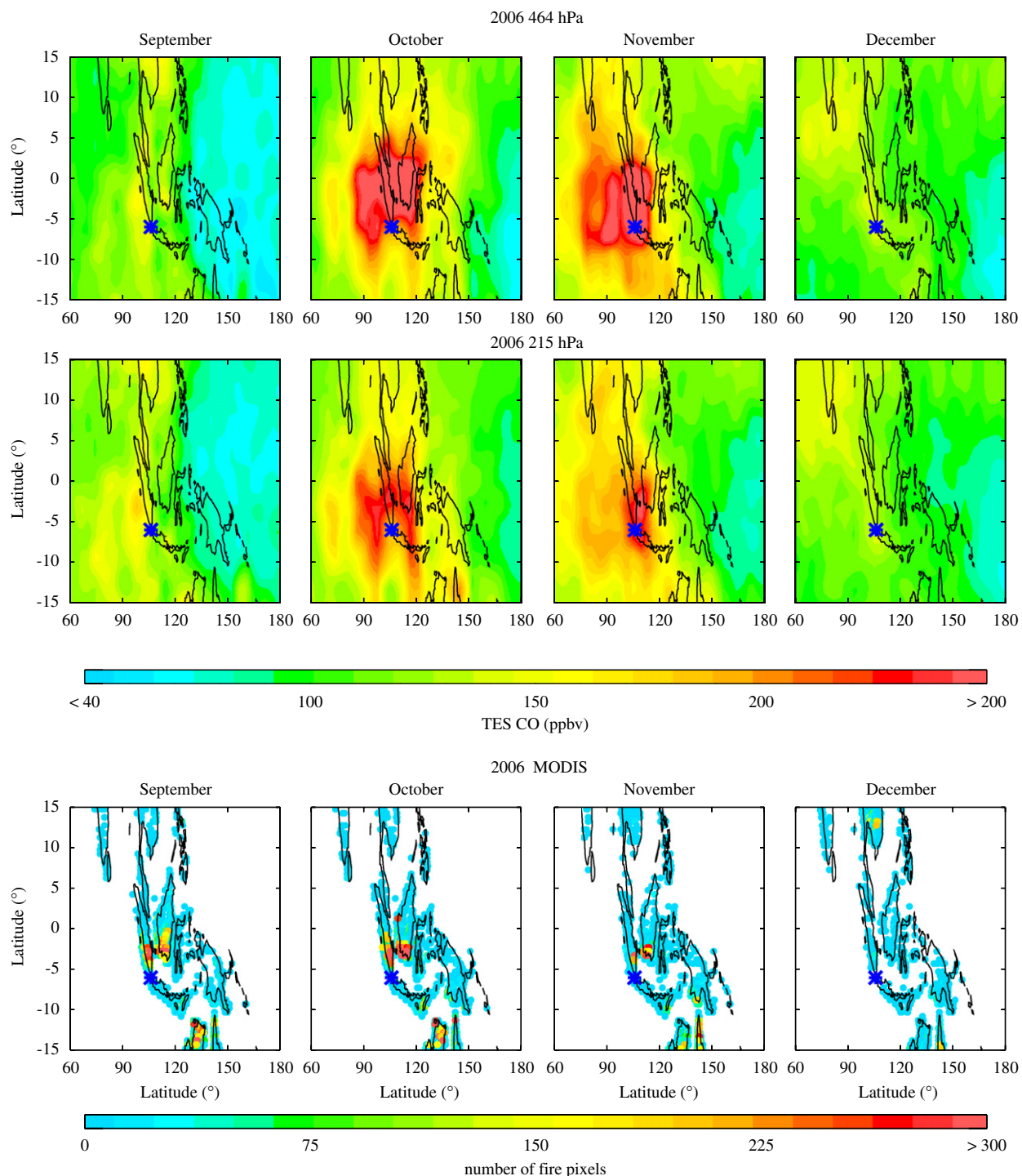
Fig. 3. TES CO monthly mean mixing ratios at 464 and 215 hPa for September to December 2006 at latitudes 15°S to 15°N and longitudes 60°E to 180°E. An asterisk is used to mark the location of Jakarta, the capitol of Indonesia. Corresponding MODIS fire counts are shown for the time period.

time periods. The right panel shows the ratio of the 2006 mixing ratios divided by the corresponding 2005 mixing ratios with the corresponding pressure levels displayed on the right axis. Ratios of October monthly averages for 2006/2005 at 200–300 hPa based on nine measurements during each year are ∼2.0. Hence, ACE

CO profiles also indicate regionally averaged CO tropospheric mixing ratios significantly higher in October 2006 than in October 2005 in the free troposphere. Fewer measurements occur at lower altitudes with only a single measurement at 5.5 km during both years with the more limited measurement set also indicating an enhancement in October 2006 relative to October 2005.

Fig. 5 (upper panel) highlights profiles of a reprocessed set of selected molecules, and near infrared extinction from occultation sr17273 (10.86°S, 86.31°E) illustrating the mixing ratios measured due to the emissions by the intense fires. The occultation was measured off the west coast of Indonesia and shows a CO mixing ratio of 268 ppbv at 9.5 km (305 hPa). The elevated upper tropospheric mixing ratios include HCN, a well-established biomass burning emission product with emissions that occur primarily during the smoldering phase of combustion [41]. The lifetime of HCN is about 5 months [46], allowing long-range transport of emissions. The back trajectories (lower panel) show the emissions are likely to have originated in the Indonesian region. Transport of emissions from distant regions for molecules such as HCN with long lifetimes will contribute in the scenes observed by ACE, though dilution reduces their contribution in the sampled airmass. The set of elevated mixing ratios of species with a range of lifetimes and near infrared extinction illustrated in this example provides evidence that the Indonesian fires were the primary source of the emissions. The measurements from the near infrared were obtained by integrating pixel measurements coincident in location and time with those of the FTS field of view.

The upper tropospheric mixing ratios of biomass burning products from the Indonesian fires are similar to those measured by ACE during intense Arctic fires during summer 2004 [47] and in the tropics during the Austral spring biomass burning season [48]. The high spectral resolution and broad infrared spectral coverage has also allowed examples of young biomass burning plumes to be identified in ACE spectra [49]. Retrievals planned for ACE version 3.0 will include additional species emitted by biomass burning including peroxyacetyl nitrate (PAN).
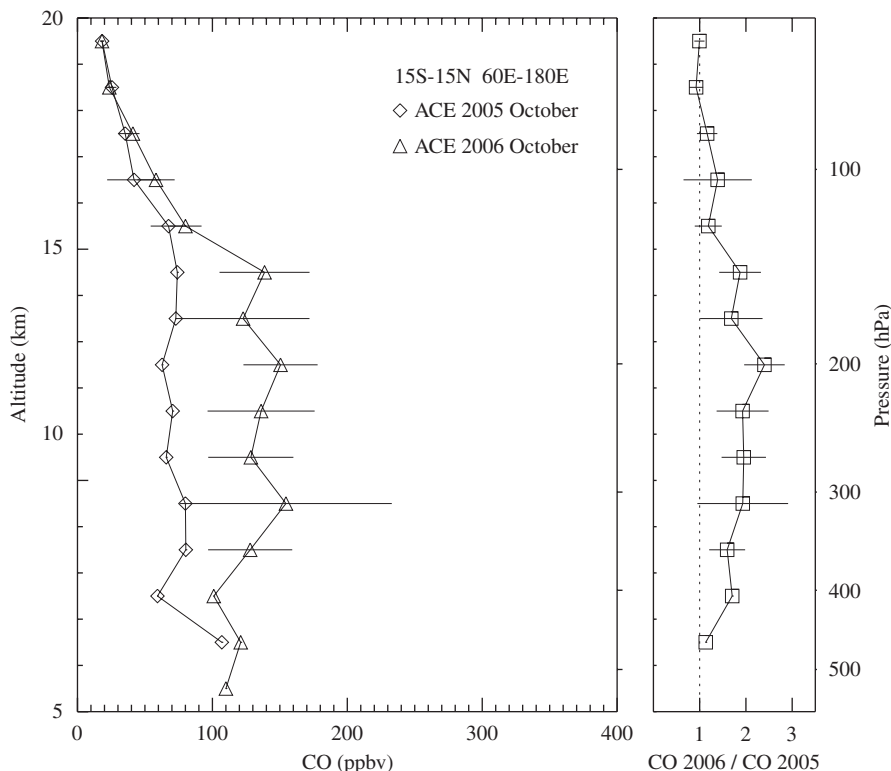
Fig. 4. ACE version 2.2 CO profiles measured during October 2005 and October 2006. Average profiles with standard deviations are displayed versus altitude in the left panels from nine occultations from 2005 and 2006. The ratio of the 2006 measurements from those from 2005 is shown in the right panels with the corresponding pressure. The number of occultations to calculate the average profile decreases with altitude for both years with to only a single occultation at the lower altitudes.
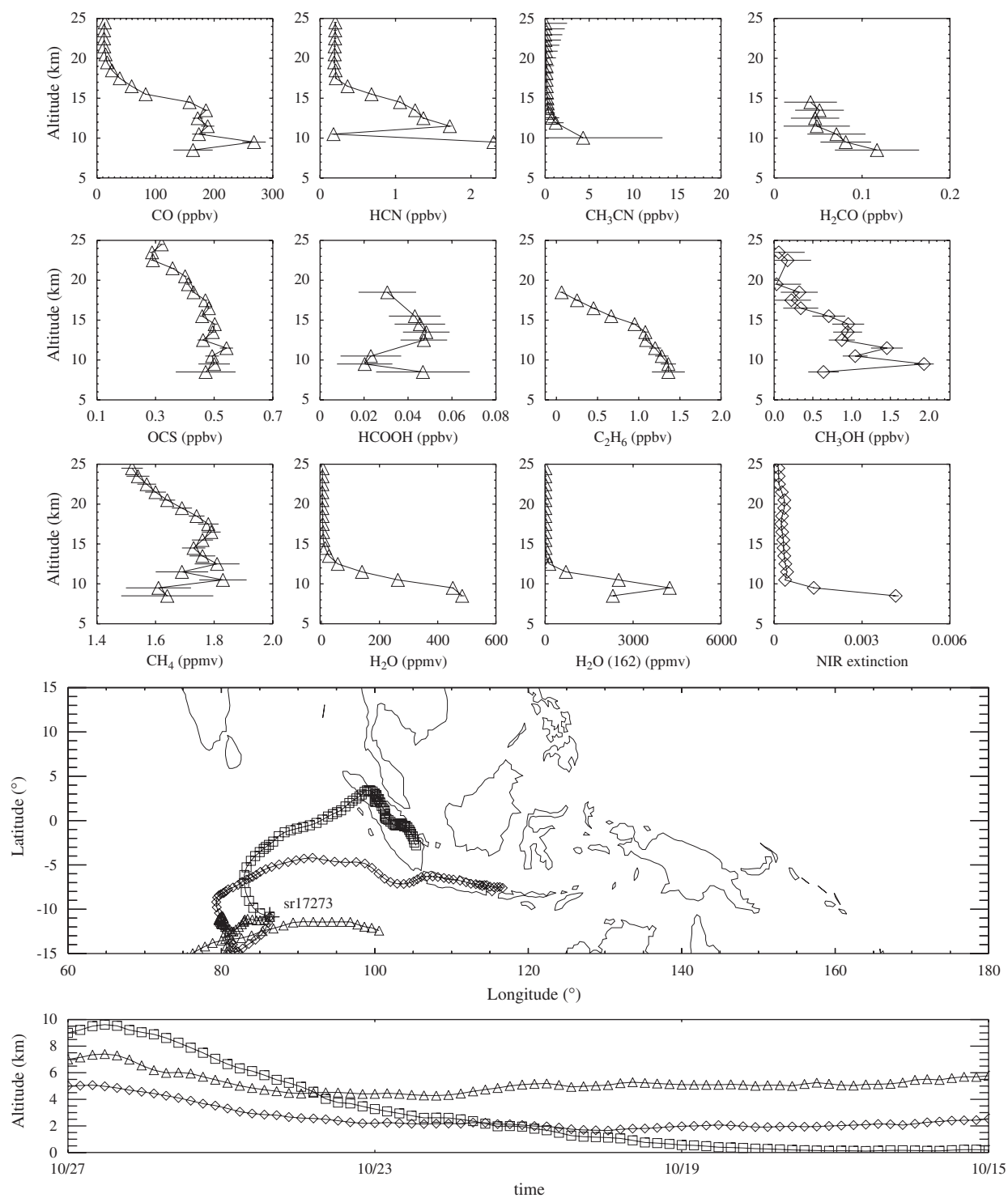
Fig. 5. Upper panel: ACE reprocessed version 2.2 measurements from occultation sr17273 (10.86°S, 86.31°E) measured on October 27, 2006. Error bars indicate the one sigma statistical uncertainty. Volume mixing ratios and extinction per km based on averages from imager pixels coincident with those of the FTS. Lower panel: altitude of backtrajectories for the location of the ACE occultation as a function of time. Initial altitudes were 5, 7, and 9 km.

5. Summary and conclusions

Monthly mean measurements of CO by TES and ACE and corresponding MODIS fire counts show a maximum in the Indonesian region during October 2006 resulted from intense and widespread peat and forest fires caused a moderate El Niño, which delayed that year's monsoon season with sharply reduced rainfall during the last quarter of 2006 that allowed wildfires across the dense tropical rainforests of Sumatra, Kalimantan, and Malaysia to spread quickly [9]. Although wildfires occur in Indonesia every year during the dry season, the rise in wildfire activity during 2006 was the worst since the intense 1997–1998 El Niño event [9] with elevated CO and tropospheric O_3 identified in the TES monthly mean fields [45]. The arrival of northeastern winter monsoons in December effectively ended the impact of the 2006 fires on the region. Higher CO mixing ratios during 2006 relative to 2005 is also supported by a comparison of ACE measurements and fire counts for the Indonsian region for the 2 years with the measurements of elevated mixing ratios of biomass burning products from ACE such as elevated HCN, C_2H_6 and HCOOH providing further evidence that the elevated emissions resulted primarily from fire emissions.

Nadir CO mixing ratios from TES global survey and step-and-stare measurements (version 2 data) have been compared with co-located ACE limb occultation measurements (version 2.2 data) in the middle and upper troposphere for the 2006 time period when TES had improved CO sensitivity [7]. The method of Rodgers and Connor [40] was used to adjust the ACE profiles with the TES averaging kernels and *a priori* constraints for the comparison. Comparison shows ACE and TES profiles with differences (ACE minus TES) for coincident measurements that agree within the uncertainties for altitudes where TES has good sensitivity. An analysis comparing ACE measurements with those from ground-based, airborne, and other satellite measurements with the goal of validating the ACE CO dataset has been submitted for publication [50]. An independent study of TES tropospheric measurements also concludes that the elevated 2006 emissions measured by TES were caused by fires in the Indonesian region [51]. As ACE measurements were obtained in both 2005 and 2006 (in addition to earlier years) with high sensitivity, the CO measurements and fire count comparison for the Indonesian region for both years provide evidence that increased 2006 emissions were related to emissions from the fires. Further understanding of the ACE and TES chemistry measurements with predictions for both sets of measurement locations will require a model that combines those measurements with other measurements (e.g., data from aircraft and surface sites combined with emission factor estimates for the measured species) and modeling of the ejection of the surface emissions to the free troposphere to provide an integrated chemical data simulation of the 2006 moderate El Niño event.

References

[1] Beer R, Glavich TA, Rider DM. Tropospheric emission spectrometer for the Earth observing systems Aura satellite. Appl Opt 2001; 40(15):2356–67.

[2] Beer R. TES on the Aura mission: scientific objectives, measurements, and analysis overview. IEEE Trans Geosci Remote Sensing 2006;44:1102–5.

[3] Bernath PF, McElroy CT, Abrams MC, Boone CD, Butler M, Camy-Peyret C, et al. Atmospheric chemistry experiment (ACE): mission overview. Geophys Res Lett 2005;32:L15S01.

[4] Boone CD, Nassar R, Walker KA, Rochon Y, McLeod SD, Rinsland CP, et al. Retrievals for the atmospheric chemistry experiment Fourier-transform spectrometer. Appl Opt 2005;44:7218–31.

[5] Carlotti M. Global-fit approach to the analysis of limb-scanning atmospheric measurements. Appl Opt 1988;27:3250–4.

[6] Rodgers CD. Inverse methods for atmospheric sounding: theory and practice. Singapore: World Scientific; 2000. 200pp.

[7] Rinsland CP, Luo M, Logan JA, Beer R, Worden H, Kulawik SS, et al. Nadir measurements of carbon monoxide (CO) distributions by the tropospheric emission spectrometer instrument onboard the Aura spacecraft: Overview of analysis approach and examples of initial results. Geophys Res Lett 2006;33:L22806.

[8] Page SE, Siegert F, Rieley JO, Boehm HD, Jaya A, Limin S. The amount of carbon released from peat and forest fires in Indonesia during 1997. Nature 2002;420:61–5.

[9] NASA, 2006. NASA data links Indonesian wildfire flare-up to recent El Niño. ⟨http://www.nasa.gov/centers/goddard/news/topstory/2007/elnino_wildfire.html⟩.

[10] Pétron G, Granier C, Khattahov B, Yudin V, Lamarque J-F, Edmonds L, et al. Monthly CO surface sources inventory based on the 2000–2001 MOPITT satellite data. Geophys Res Lett 2004;31:L21107.

[11] Levy II H. Normal atmosphere: large radical and formaldehyde concentrations predicted. Science 1971;173:141–3.

[12] Thompson AM. The oxidizing capacity of the earth's atmosphere: probable past and future changes. Science 1992;256:1157–65.

[13] Holloway T, Levy II H, Kasibharla PK. Global distribution of carbon monoxide. J Geophys Res 2000;105:12123–47.

[14] Logan J, Prather MJ, Wofsy SC, McElroy MB. Tropospheric chemistry: a global perspective. J Geophys Res 1981;86:7210–54.

[15] Pergamaschi P, Hein R, Heinmann M, Crutzen PJ. Inverse modeling of the global CO cycle 1. Inversion of CO mixing ratios. J Geophys Res 2000;105:1909–27.

[16] Rinsland CP, Levine JS. Free tropospheric carbon monoxide concentrations in 1950–1951 deduced from infrared total column amount measurements. Nature 1985;318:250–4.

[17] Deeter MN, Edmonds LK, Francis GL, Edwards DP, Gille GC, Warner JX, et al. Operational carbon monoxide retrieval algorithm and selected results for the MOPITT instrument. J Geophys Res 2003;108:L15112.

[18] Deeter MN, Edmonds LK, Edwards DP, Gille GC. Vertical resolution and information content of CO profiles retrieved by MOPITT. Geophys Res Lett 2004;31:L15112.

[19] Edwards DP, Edmonds LK, Hauglustaine DA, Chu DA, Gille JC, Kaufman YJ, et al. Observations of carbon monoxide and aerosols from the Terra satellite: Northern hemisphere variability. J Geophys Res 2004;109:D24202.

[20] Aumann HH, Chahine M, Gautier C, Goldberg MD, Kalnay E, McMillin LM, et al. AIRS/AMSU/HSB on the Aqua mission: design, science objectives, data products, and processing systems. IEEE Trans Geosci Remote Sensing 2003;41:253–64.

[21] McMillan WW, Barnet C, Strow L, Chanine MT, McCourt ML, Warner JX, et al. Daily global maps of carbon monoxide from NASA's atmospheric infrared sounder. Geophys Res Lett 2005;32:L11801.

[22] Buchwitz M, Rozanov V, Burrows J. A near-infrared optimized DOAS method for the fast global retrieval of atmospheric CH_4, CO, CO_2, H_2O, and N_2O total column amounts from SCIAMACHY ENVISAT-1 nadir radiances. J Geophys Res 2000;105:15231–45.

[23] Buchwitz M, Beek R, Bramstedt K, Nöl S, Bovensmann J, Burrows J. Global carbon monoxide as retrieved from SCIAMACHY by WFM-DOAS. Atmos Chem Phys 2004:1945–60.

[24] Frankenberg C, Platt U, Wagner T. Retrieval of CO from SCIAMACHY onboard ENVISAT: detection of strongly polluted areas and seasonal patterns in global CO abundances. Atmos Chem Phys 2005;5:1639–44.

[25] Belotti C, Carli, B, Ceccherini S, Del Bianco SD, Jin J, Raspollini P. Retrieval of tropospheric carbon monoxide from MIPAS measurements, ESA Atmospheric Sciences Conference, 8–12 May 2006, Frasciti, Italy.

[26] Filipiak MJ, Harwood RS, Jiang J, Li Q, Livesay NJ, Manney GL, et al. Carbon monoxide measured by EOS MLS on Aura: first results. Geophys Res Lett 2005;32:L14825.

[27] Froidevaux L, Livesay NJ, Read WG, Jiang YB, Jiminez C, Filipiak MJ, et al. Early validation analyses of atmospheric profiles from EOS MLS on the Aura satellite. IEEE transactions Geosci Remote Sensing 2006;44:1106–21.

[28] Turquety S, Hadji-Lazaro J, Clerbaux C, Hauglustaine DA, Clough SA, Cassé V, et al. Operational trace gas retrieval algorithm for the infrared atmospheric sounding interferometer. J Geophys Res 2004;109:D21301.

[29] Schoeberl MR, Douglass AR, Hilsenrath EH, Bhartia PK, Beer R, Waters JW, et al. Overview of the EOS Aura mission. IEEE Trans Geosci Remote Sensing 2006;44:1066–74.

[30] Worden J, Kulawik SS, Shephard MW, Clough SA, Worden H, Bowman K, et al. Predicted errors of tropospheric emission spectrometer nadir retrievals from spectral window selection. J Geophys Res 2004;109:D09308.

[31] Clough SA, Shephard MW, Worden J, Brown PD, Worden HM, Luo M, et al. Forward model and Jacobians for tropospheric emission spectrometer retrievals. IEEE Trans Geosci Remote Sensing 2006;44:1308–23.

[32] Bowman KW, Rodgers CD, Kulawik SS, Worden J, Sarkissian E, Osterman G, et al. Tropospheric emission spectrometer: retrieval method and error analysis. IEEE Trans Geosci Remote Sensing 2006;44:1297–307.

[33] Kulawik SS, Osterman G, Jones DBA, Bowman KW. Calculation of altitude-dependent Tikhonov constraints for TES nadir retrievals. IEEE Trans Geosci Remote Sensing 2006;44:1334–42.

[34] Norton R, Beer R. New apodizing functions for Fourier spectrometry. J Opt Soc Am 1976;66:259–64.

[35] Kulawik SS, Worden J, Eldering A, Bowman K, Gunson M, Osterman JB, et al. Implementation of cloud retrievals for tropospheric emission spectrometer (TES) atmospheric retrievals-part I description and characterization of errors on trace gas retrievals. J Geophys Res 2006;111:D24204.

[36] Rothman LS, Barbe A, Benner DC, Brown LR, Camy-Peyret C, Carleer MR, et al. The HITRAN molecular spectroscopic database: edition of 2000 including updates through 2001. JQSRT 2003;82:5–44.

[37] Rothman LS, Jacquemart D, Barbe A, Benner DC, Birk M, Brown LR, et al. The HITRAN 2004 molecular spectroscopy database. JQSRT 2005;96:139–204.

[38] Brasseur GP, Hauglustaine DA, Walters S, Rasch PJ, Müller J-F, Granier C, et al. MOZART: a global chemical transport model for ozone and related chemical tracers, Part 1: Model description. J Geophys Res 1998;103:28,265–89.

[39] Luo M, Rinsland CP, Rodgers CD, Logan JA, Worden H, Kulawich S, et al. Comparison of carbon monoxide measurements by TES and MOPITT-the influence of *a priori* data and instrument characteristics on nadir atmospheric species retrievals. J Geophys Res 2007;112(D9):D09303.

[40] Rodgers CD, Connor BJ. Intercomparisons of remote sounding instruments. J Geophys Res 2003;108:4116.

[41] Rinsland CP, Gunson MR, Wang P-H, Arduini RF, Baum BA, Minnis P, et al. ATMOS/ATLAS 3 infrared profile measurements of trace gases in the tropical and subtropical upper troposphere. JQSRT 1998;60:891–901.

[42] Wang P-H. SAGE II tropospheric measurement frequency and its meteorological implication. In: Proceedings of the Seventh Conference on Satellite Meteorology and Oceanography. Boston: American Meteorological Society; 1994. p. J15–8.

[43] Clerbaux C, Coheur P-F, Hurtmans D, Barret B, Carleer M, Colin R, et al. Carbon monoxide distribution from the ACE-FTS solar occultation measurements. Geophys Res Lett 2005;32:L16S01.

[44] Luo M, Rinsland C, Fisher B, Sachse G, Diskin G, Logan J, Worden H, Kulawik S, Osterman G, Eldering A, Herman R, Shephard M. TES carbon monoxide validation with DACOM aircraft measurements during INTEX-B 2006. J Geophys Res 2007;112:D24S48, doi:10.1029/2007JD008803.

[45] Luo M, Richards N. Tropospheric ozone and CO monthly mean fields from TES and the GEOS CHEM model 2006. Fall AGU meeting, San Francisco, CA, paper A31B-0877.

[46] Singh HB, Salas L, Herlth D, Kolyer R, Cyech E, Viezee W, et al. In situ measurements of HCN and CH_3CN in the Pacific troposphere: sources, sinks, and comparisons with spectroscopic observations. J Geophys Res 2003;108:8795.

[47] Rinsland CP, Dufour G, Boone CD, Bernath PF, Chiou L, Coheur P, et al. Satellite boreal measurements over Alaska and Canada during June–July 2004: simultaneous measurements of upper tropospheric CO, C_2H_6, HCN, CH_3Cl, CH_4, C_2H_2, CH_3OH, HCOOH, OCS, and SF_6 mixing ratios. Global Biogeochem Cycles 2007;21:GB3008.

[48] Rinsland CP, Dufour G, Boone CD, Bernath PF, Chiou L. Atmospheric chemistry experiment (ACE) measurements of elevated southern hemisphere upper tropospheric CO, C_2H_6, HCN, and C_2H_2 mixing ratios from biomass burning emissions and long-range transport. Geophys Res Lett 2005;32:L208303.

[49] Coheur P, Herbin H, Clerbaux C, Hurtmans D, Wespes C, Carleer M, et al. ACE-FTS observation of a young biomass burning plume: first reported measurements of C_2H_4, C_3H_6O, H_2CO, and PAN by infrared solar occultation from space. Atmos Chem Phys Discuss 2007;7:7907–32.

[50] Clerbaux C, George M, Turquety S, Walker KA, Barret B, Bernath P, et al. CO measurements from the ACE FTS satellite instrument: data analysis and validation using ground-based, airborne, and spaceborne observations. Atmos Chem Phys Discuss 2007;7:15277–340.

[51] Logan JA, Megretskaia I, Nassar R, Murray LT, Zhang L, Bowman KW, et al. The effects of the 2006 El Niño on tropospheric composition as revealed by data from the Tropospheric Emission Spectrometer (TES). Geophy Res Lett 2008; in press.